

# Unique X-ray Sheet Structure of 1,8-Bis(imidazolium) Anthracene and Its Application as a Fluorescent Probe for DNA and DNase

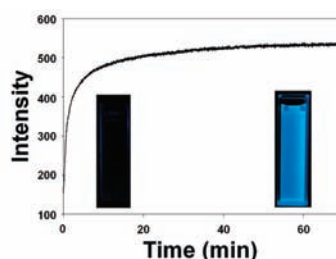
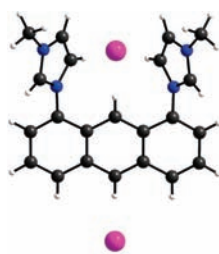
Ha Na Kim,<sup>†</sup> Jisoo Lim,<sup>‡</sup> Han Na Lee,<sup>†</sup> Ju-Woo Ryu,<sup>§</sup> Min Jung Kim,<sup>†</sup> Joohee Lee,<sup>‡</sup> Dong-Ung Lee,<sup>§</sup> Youngmee Kim,<sup>†</sup> Sung-Jin Kim,<sup>†</sup> Kap Duk Lee,<sup>\*,§</sup> Hee-Seung Lee,<sup>\*,‡</sup> and Juyoung Yoon<sup>\*,†,||</sup>

Department of Chemistry and Nano Science, Ewha Womans University, Seoul 120-750, Korea, Molecular-Level Interface Research Center, Department of Chemistry, KAIST, Daejeon 305-701, Korea, Department of Chemistry, Dongguk University, Kyungju, Kyungbuk 780-714, Korea, and Department of Bioinspired Science (WCU), Ewha Womans University, Seoul 120-750, Korea

jyoon@ewha.ac.kr; hee-seung\_lee@kaist.ac.kr; kdlee@dongguk.ac.kr

Received December 29, 2010

## ABSTRACT



A new imidazolium anthracene derivative **1** was synthesized, and its unique X-ray crystal structure was examined. In aqueous solutions, probe **1** exhibited a selective fluorescent quenching effect only with DNA among various anions including the nucleotides investigated. This probe was further applied to monitor the activity of DNase.

Among the various types of anion selective probes,<sup>1</sup> imidazolium-based sensors have been studied extensively in recent years.<sup>2</sup> Imidazolium salts can be formed from protonation or substitution at the nitrogen atom of imidazole where the positive charge is delocalized in the imidazole ring. In imidazolium-based anion receptors, charge–charge electrostatic interaction dominates. This novel type of charged hydrogen bonding is quite different and intriguing compared to many other conventional hydrogen bonds. Although a range of anionic targets including GTP<sup>3</sup> and ATP<sup>4</sup> by imidazolium based sensors has been investigated, there is only one report on DNA sensing so far.<sup>5</sup>

The recognition and sensing of DNA is of paramount importance because increasing evidence has shown that various diseases are caused by genetic disorders, and DNA measurements will be helpful for diagnosis. In addition, electron and energy transfer in DNA has attracted additional interest.<sup>6</sup> Accordingly, considerable attention has been devoted to the development of new fluorescent probes for DNA.<sup>7</sup>

In this paper, we synthesized a new imidazolium–anthracene derivative **1**, in which the imidazolium moiety is directly linked to anthracene. The iodide form (**2**) showed a

<sup>†</sup> Department of Chemistry and Nano Science, Ewha Womans University.

<sup>‡</sup> KAIST.

<sup>§</sup> Dongguk University.

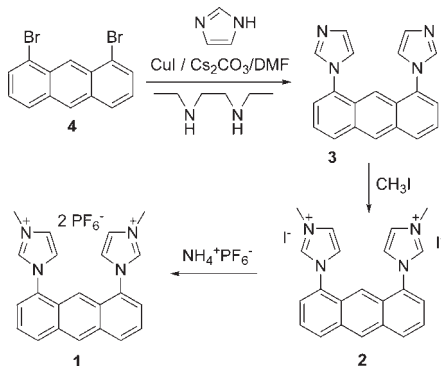
<sup>||</sup> Department of Bioinspired Science (WCU), Ewha Womans University.

(1) (a) Martínez-Máñez, R.; Sancenón, F. *Chem. Rev.* **2003**, *103*, 4419. (b) Gunnlaugsson, T.; Glynn, M.; Tocci, G. M.; Kruger, P. E.; Pfeffer, F. M. *Coord. Chem. Rev.* **2006**, *250*, 3094. (c) Kim, S. K.; Lee, D. H.; Hong, J.-I.; Yoon, J. *Acc. Chem. Res.* **2009**, *42*, 23. (d) Xu, Z.; Chen, X.; Kim, H. N.; Yoon, J. *Chem. Soc. Rev.* **2010**, *39*, 127. (e) Li, A.-F.; Wang, J.-H.; Wang, F.; Jiang, Y.-B. *Chem. Soc. Rev.* **2010**, *39*, 3729.

unique X-ray structure. Probe **1** was applied successfully for sensing CT DNA and monitoring the activity of DNase.

For the synthesis of probe **1**, 1,8-dibromoanthracene **4** was synthesized from 1,8-dichloroanthraquinone in two steps according to the reported procedures.<sup>8</sup> 1,8-Bisimidazolyl anthracene **3** was synthesized by the treatment of 1,8-dibromoanthracene **4** with imidazole in the presence of copper iodide, cesium carbonate, and *N,N'*-diethylethylenediamine in 17% yield after column chromatography using ethyl acetate–methanol (3:1, v/v), as shown in Scheme 1. A reaction with methyl iodide afforded the iodide salt form of 1,8-bis(imidazolium) anthracene **2** in 95% yield, which was then converted to its phosphorus hexafluoride salt **1**. The characterization data for these new compounds and detailed procedures are presented in the Supporting Information.

### Scheme 1. Synthesis of Fluorescent Probe **1**



Since two imidazolium groups were introduced to the 1,8-positions of anthracene without any linker for the first time, it is interesting to know how these imidazolium rings are located. Fortunately, the crystal structure of compound **2** could be obtained, which displayed a unique sheet structure, as shown in Figure 1. As shown in Figure 1a, there is a mirror plane through C9/C10 and I1/I2.

(2) (a) For a review paper, see: Xu, Z.; Kim, S. K.; Yoon, J. *Chem. Soc. Rev.* **2010**, *39*, 1457. (b) Yoon, J.; Kim, S. K.; Singh, N. J.; Kim, K. S. *Chem. Soc. Rev.* **2006**, *35*, 355. (c) Sato, K.; Arai, S.; Yamagishi, T. *Tetrahedron Lett.* **1999**, *40*, 5219. (d) Kim, S. K.; Singh, N. J.; Kim, S. J.; Kim, H. G.; Kim, J. K.; Lee, J. W.; Kim, K. S.; Yoon, J. *Org. Lett.* **2003**, *5*, 2083. (e) Kim, S. K.; Kang, B.-G.; Koh, H. S.; Yoon, Y.-J.; Jung, S. J.; Jeong, B.; Lee, K.-D.; Yoon, J. *Org. Lett.* **2004**, *6*, 4655. (f) Kim, S. K.; Singh, N. J.; Kwon, J.; Hwang, I.-C.; Park, S. J.; Kim, K. S.; Yoon, J. *Tetrahedron* **2006**, *62*, 6065. (g) Coll, C.; Casasús, R.; Martínez-Máñez, R.; Marcos, M. D.; Sancenón, F.; Soto, J. *Angew. Chem., Int. Ed.* **2007**, *46*, 1675. (h) Lu, Q.-S.; Dong, L.; Zhang, J.; Li, J.; Jiang, L.; Huang, Y.; Qin, S.; Hu, C.-W.; Yu, X.-Q. *Org. Lett.* **2009**, *11*, 669. (i) Kumar, S.; Luxami, V.; Kumar, A. *Org. Lett.* **2008**, *10*, 5549. (j) Amendola, V.; Boiocchi, M.; Colasson, B.; Fabbrizzi, L.; Monzani, E.; Douton-Rodriguez, M.-J.; Spadini, C. *Inorg. Chem.* **2008**, *47*, 4808. (k) Xu, Z.; Kim, S. K.; Han, S. J.; Lee, C.; Kociok-Kohn, G.; James, T. D.; Yoon, J. *Eur. J. Org. Chem.* **2009**, 3058. (l) Gong, H. Y.; Rambo, B. M.; Karnas, E.; Lynch, V. M.; Sessler, J. L. *Nat. Chem.* **2010**, *2*, 406. (m) Chen, X.; Kang, S.; Kim, M. J.; Kim, J.; Lim, Y. S.; Kim, H.; Chi, B.; Kim, S.-J.; Lee, J. Y.; Yoon, J. *Angew. Chem., Int. Ed.* **2010**, *49*, 1422. (n) Kim, S. K.; Singh, N. J.; Kwon, J.; Hwang, I.-C.; Park, S. J.; Kim, K. S.; Yoon, J. *Tetrahedron* **2006**, *62*, 6065. (o) Xu, Z.; Singh, N. J.; Kim, S. K.; Spring, D. R.; Kim, K. S.; Yoon, J. *Chem.–Eur. J.* **2011**, *17*, 1163.

(3) Kwon, J. Y.; Singh, N. J.; Kim, H.; Kim, S. K.; Kim, K. S.; Yoon, J. *J. Am. Chem. Soc.* **2004**, *126*, 8892.

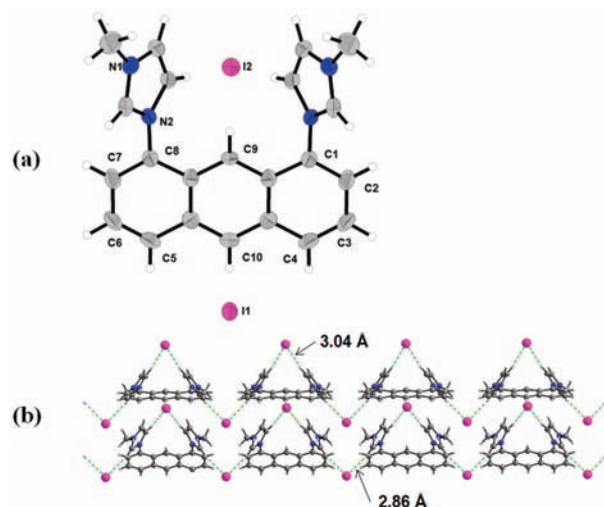


**Figure 1.** (a) X-ray crystal structure of **2** (Blue: N atom; Pink: I atom). (b) One-dimensional structure through nonclassical hydrogen bonding interactions.

Nonclassical hydrogen bonding interactions<sup>9</sup> between the iodides and imidazolium hydrogen ( $H_a/H_b$  in Figure 2) atoms produce an interesting one-dimensional chain structure, as shown in Figure 1b. Interestingly, the central C–H of the imidazolium groups on the 1,8-position of anthracene face outward, probably due to the steric problem of the C9–H( $H_d$ ) of anthracene. The dihedral angle between the anthracene moiety and imidazolium ring was 52.45°.

Based on the 2D COSY and 2D NOESY (Supporting Information) in DMSO-*d*<sub>6</sub>, the aromatic protons of compound **1** were assigned, as shown in Figure 2. Interestingly, the C9–H peak of anthracene ( $H_d$ ) appeared at 8.13, which is shifted upfield compared to those of other anthracene derivatives. This can be attributed to the closely located imidazolium rings. Unlike the crystal structure, rotation of the imidazolium rings can occur at room temperature to some extent because the cross peak of  $H_b$  and  $H_e$  was observed on the NOESY spectrum. The <sup>1</sup>H

(4) Xu, Z.; Singh, N. J.; Lim, J.; Pan, J.; Kim, H. N.; Park, S.; Kim, K. S.; Yoon, J. *J. Am. Chem. Soc.* **2009**, *131*, 15528.

(5) Neelakandan, P. P.; Ramaiah, D. *Angew. Chem., Int. Ed.* **2008**, *47*, 8407.

(6) (a) Venkatesan, N.; Seo, Y. J.; Kim, B. H. *Chem. Soc. Rev.* **2008**, *37*, 648. (b) Tsui, C.; Coleman, L. E.; Griffith, J. L.; Bennett, E. A.; Goodson, S. G.; Scott, J. D.; Pittard, W. S.; Devine, S. E. *Nucleic Acids Res.* **2003**, *31*, 4910.

(7) (a) Kumar, C.; Asuncion, E. H. *Chem. Commun.* **1999**, 1219. (b) Kumar, C. V.; Punzalan, E. H. A.; Tan, W. B. *Tetrahedron* **2000**, *56*, 7027. (c) Seo, Y. S.; Ryu, J. H.; Kim, B. H. *Org. Lett.* **2005**, *7*, 4931. (d) Horowitz, E. D.; Hud, N. V. *J. Am. Chem. Soc.* **2006**, *128*, 15380. (e) Wang, S.; Gaylord, B. S.; Bazan, G. C. *J. Am. Chem. Soc.* **2004**, *126*, 5446. (f) Seo, Y. J.; Rhee, H.; Joo, T.; Kim, B. H. *J. Am. Chem. Soc.* **2007**, *129*, 5244. (g) Menacher, F.; Rubner, M.; Berndt, S.; Wagenknecht, H. A. *J. Org. Chem.* **2008**, *73*, 4263. (h) Yang, Y.; Ji, S.; Zhou, F.; Zhao, J. *Biosens. Bioelectron.* **2009**, *24*, 3442. (i) Lee, I. J.; Yi, J. W.; Kim, B. H. *Chem. Commun.* **2009**, 5383.

(8) (a) Benites, M. d. R.; Fronczek, F. R.; Hammer, R. P.; Maverick, A. W. *Inorg. Chem.* **1997**, *36*, 5826. (b) Haenel, M. W.; Jakubik, D.; Krüger, C.; Betz, P. *Chem. Ber.* **1991**, *124*, 333.

(9) Steiner, Th. *Cryst. Rev.* **1996**, *6*, 1–57.

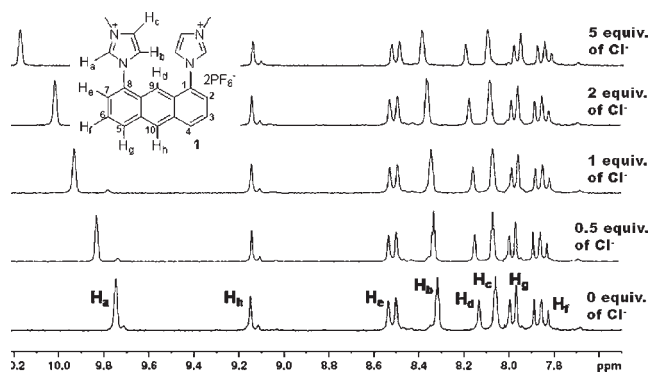


**Figure 2.** Partial  $^1\text{H}$  NMR spectra of **1** (2 mM) in  $\text{DMSO-}d_6$  with the addition of tetrabutylammonium chloride.

NMR data of compound **2** showed a similar pattern. As shown in Figure 2, only imidazolium  $\text{H}_a$  of compound **1** displayed large downfield shifts from 9.75 to 10.18 ppm (5 equiv of  $\text{Cl}^-$ ) in  $\text{DMSO-}d_6$  upon the addition of  $\text{Cl}^-$ . There were relatively small downfield shifts for  $\text{H}_b$  ( $\Delta\delta = 0.08$  ppm),  $\text{H}_d$  ( $\Delta\delta = 0.07$  ppm), and  $\text{H}_c$  ( $\Delta\delta = 0.04$  ppm) and no significant change in the chemical shifts of the other aromatic hydrogens.

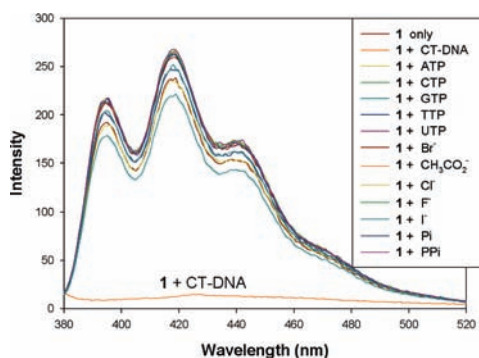


**Figure 3.** Fluorescent changes of **1** ( $3 \mu\text{M}$ ) with various anions (100 equiv) and CT DNA (10 equiv) in 10 mM sodium phosphate buffer (5%  $\text{CH}_3\text{CN}$ ) at pH 7 (excitation at 368 nm).

In 100% acetonitrile, compound **1** showed typical fluorescent quenching effects with anions as shown in the Supporting Information (Figure S4). Especially,  $\text{H}_2\text{PO}_4^-$  and pyrophosphate displayed large fluorescent quenching effects. To examine the binding properties in aqueous solution, the fluorescent changes in compound **1** toward various anions were examined at pH 7.4 (10 mM sodium phosphate buffer (5%  $\text{CH}_3\text{CN}$ )). Compound **1** ( $6 \mu\text{M}$ ) did not display any fluorescent changes with various anions, such as  $\text{F}^-$ ,  $\text{Cl}^-$ ,  $\text{Br}^-$ ,  $\text{I}^-$ ,  $\text{CH}_3\text{CO}_2^-$ ,  $\text{HSO}_4^-$ ,  $\text{H}_2\text{PO}_4^-$ , pyrophosphate, ATP, CTP, GTP, TTP, and UTP (Figure 3). These results encouraged us to check the fluorescent changes in compound **1** with DNA. Indeed, compound **1** exhibited a large and selective fluorescent quenching effect with the CT

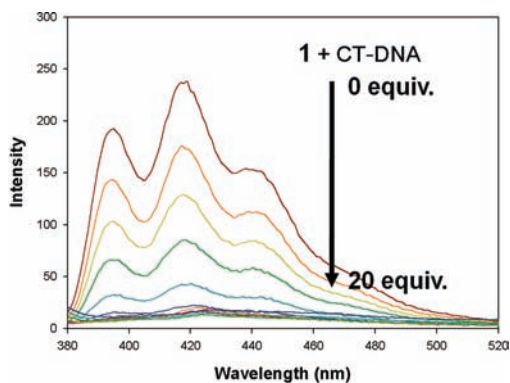


**Figure 4.** Fluorescent titrations of **1** ( $3 \mu\text{M}$ ) with CT DNA (0.01, 0.04, 0.08, 0.1, 0.4, 0.7, 0.9, 1, 3, 5, 10, and 20 equiv) in 10 mM sodium phosphate (5%  $\text{CH}_3\text{CN}$ ) at pH 7 (excitation at 368 nm).

DNA duplex (Figure 3). The optical change upon addition of the CT DNA duplex was more than 10-fold.

The fluorescence intensity and UV absorption spectra of probe **1** decreased with increasing concentration of calf thymus DNA (Figures 4 and S4), and the association constant was calculated to be  $8.9 \times 10^6 \text{ M}^{-1}$ . The probe was compared with the commercially available intercalating agent Proflavine, which displayed a similar fluorescent quenching effect (Figure S5A).

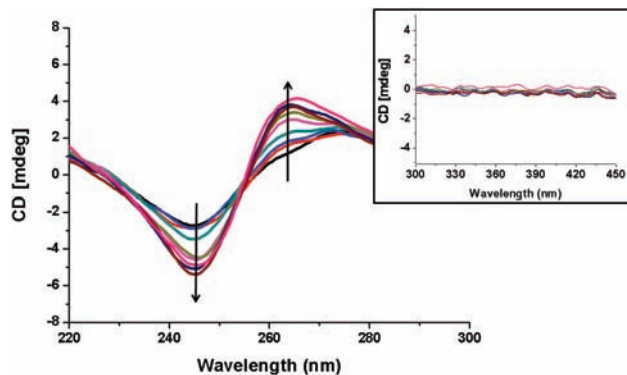


**Figure 5.** Circular dichroism of calf thymus DNA ( $60 \mu\text{M}$ ) with probe **1**;  $[\mathbf{1}]/[\text{CT DNA}]$  ratios = 0.05, 0.1, 0.2, 0.3, 0.5, 0.7, 1, 1.5, 2. Inset: CD spectrum of CT DNA at 300–450 nm wavelength.

Circular dichroism (CD) was also used to consider the binding mechanism.<sup>10</sup> Similar CD spectra usually represent a similar binding mode between the probe and nucleic acid.<sup>11</sup> The effect of probe **1** on the CD of CT DNA is shown in Figure 5. The CD spectra of CT DNA exhibit the maximum band at 245 nm (negative) and 275 nm

(10) (a) Kim, H.-K.; Kim, J.-M.; Kim, S. K.; Rodger, A.; Nordén, B. *Biochemistry* **1996**, *35*, 1187. (b) Lyng, R.; Hard, T.; Nordén, B. *Biopolymers* **1987**, *26*, 1327.

(11) Horowitz, E. D.; Hud, N. V. *J. Am. Chem. Soc.* **2006**, *128*, 15380.

(positive), respectively. Those spectra were altered to the enhancement of the positive and negative signal with increasing ratio of probe/CT DNA. Under the same conditions, a somewhat larger CD band of Proflavine with calf thymus DNA was observed, but the signal band of probe **1** was similar to that of Proflavine (Figure-S5). In addition, intercalating agents generally show no induced CD (ICD) or a weak negative signal in the absorption band<sup>12</sup> and there was no ICD in the 360–400 nm regions (Figure 5, inset), which is the range of the absorption of probe **1**. Therefore, the results suggest that the binding mode of probe **1** can be intercalative.

As described in our previous paper, there might be ionic hydrogen bonding interactions between phosphate oxygens and imidazolium groups in anthracene, and this interaction can help strengthen the binding of probe **1** to CT DNA.<sup>4</sup> The effect of the ionic strength in the presence of the increasing NaCl concentration is illustrated in Figure S6. The NaCl concentration has relatively little effect on the emission intensity of the probe with CT DNA. The buffer solutions used for all of the CT DNA experiments contain 100 mM of NaCl. The quenching effect by CT DNA on the probe and the disturbed CD spectrum of CT DNA by the probe are evidence that the major interaction of the probe with CT DNA was intercalation.

Probe **1** was then utilized as a fluorescent sensor for monitoring the activity of DNase. The hydrolysis of CT DNA with DNase in the presence of Mg<sup>2+</sup> can be monitored by the revival of fluorescence of probe **1** as shown in Figure 6. Within 10 min, the hydrolysis of CT DNA was completed. These results demonstrate that probe **1** can be used to monitor the enzyme activity and hydrolysis process. Since the fluorescent quenching was very effective with CT DNA compared to that of Proflavine, the hydrolysis by DNase induced a nice “turn-on” signal.

In conclusion, a new bis(imidazolium) anthracene was synthesized, in which two imidazolium groups were introduced to the 1- and 8-positions of anthracene without a

(12) Janovec, L.; Sabolová, D.; Kožurková, M.; Paulíková, H.; Kristian, P.; Ungvarský, J.; Moravíková, E.; Bajdichová, M.; Podhradský, D.; Imrich, J. *Bioconjugate Chem.* **2007**, *18*, 93.

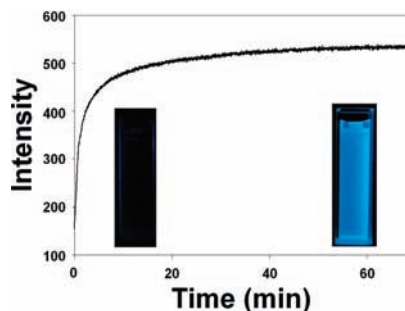


**Figure 6.** Hydrolysis diagram of DNA (60  $\mu$ M) with DNase (25  $\mu$ g/mL) in the presence of probe **1** (3  $\mu$ M) and Mg(ClO<sub>4</sub>)<sub>2</sub> (300  $\mu$ M) (excitation at 368 nm; emission at 418 nm; slit: 3.0, 5.0 nm, respectively).

linker for the first time. The X-ray crystal structure of the iodide salt form revealed a unique sheet pattern. Typical ionic hydrogen bonding and nonclassical hydrogen bonding were observed between the imidazolium hydrogens and iodide.

Probe **1** was applied successfully for sensing CT DNA and monitoring the activity of DNase. In an aqueous solution, probe **1** displayed a selective fluorescent quenching effect with CT-DNA among the various anions and nucleotides examined. Furthermore, probe **1** displayed “Off–On” fluorescent changes with DNase.

**Acknowledgment.** J.Y. acknowledges a National Research Foundation (NRF) grant (20100018895, 201000-01481) and WCU (R31-2008-000-10010-0). H.S.L. acknowledges a Basic Research Promotion Fund (KRF-2005-205-C00043) and National Research Foundation (NRF) grant (2010-0001953).

**Supporting Information Available.** Experimental procedures and characterization data of compounds have been described in the Supporting Information. This material is available free of charge via the Internet at <http://pubs.acs.org>.